Standard model Higgs boson-inflaton and dark matter

T. E. Clark,[*] Boyang Liu,[†] and S. T. Love[‡]

Department of Physics, Purdue University, West Lafayette, Indiana 47907-2036, USA

T. ter Veldhuis[§]

Department of Physics & Astronomy, Macalester College, Saint Paul, Minnesota 55105-1899, USA

The standard model Higgs boson can serve as the inflaton field of slow roll inflationary models provided it exhibits a large nonminimal coupling with the gravitational scalar curvature. The Higgs boson self interactions and its couplings with a standard model singlet scalar serving as the source of dark matter are then subject to cosmological constraints. These bounds, which can be more stringent than those arising from vacuum stability and perturbative triviality alone, still allow values for the Higgs boson mass which should be accessible at the LHC. As the Higgs boson coupling to the dark matter strengthens, lower values of the Higgs boson mass consistent with the cosmological data are allowed.

I. INTRODUCTION

The inflationary paradigm has proven extremely successful in accounting for a wealth of cosmological observations. It not only explains the large scale homogeneity and isotropy of the present universe, but also accounts for the generation of the nearly scale invariant primordial perturbations responsible for structure formation [1]. The implementation of the slow roll inflation is generally achieved by the inclusion of an independent scalar degree of freedom, the inflaton. It is tempting to try to identify the inflaton with the standard model Higgs field, h, with a λh^4 potential. Unfortunately, early attempts at such an identification were plagued [2] by the required flatness of the inflaton potential which is dictated by the size of the observed density fluctuations. This in turn necessitated far too small a quartic self-coupling for the inflaton for it to be identified with the Higgs scalar. However, by including a nonminimal coupling of the Higgs doublet, H, to the gravitational Ricci scalar curvature, R, with a large coupling constant $\xi \sim 10^3$–10^4, it has been argued [3–15] the resultant Higgs potential can indeed be flat enough for it to play the additional role of the inflaton. In such a case, the shape of the Higgs-inflaton effective potential in the inflationary region allows for a range of cosmologically acceptable values for the Higgs boson mass even after the inclusion of radiative corrections. As such, slow roll inflation can be implemented without the need for additional degrees of freedom already appearing in the minimal standard model.

The presence of nonbaryonic dark matter, however, does require the inclusion of additional degrees of freedom beyond those appearing in the standard model. A minimal extension of the standard model which accounts for this dark matter is the inclusion of a singlet Hermitian scalar field, S, [16–19]. This simple, and clearly minimal, extension can account for the correct abundance of dark matter. Its lack of direct [20] and indirect [21,22] detection or observation at high energy accelerators [23–25] have already somewhat constrained the model's parameter space, and experiments in the near future will further probe its validity. For a dark matter scalar mass m_S near half the Higgs boson mass, the dark matter annihilation process via an intermediate Higgs boson line becomes resonant. Because of this efficient process, the dark matter remains in thermodynamic equilibrium longer (to a lower temperature) and consequently the relic density is too low unless the Higgs boson to dark matter coupling κ is quite small. On the other hand, for scalar dark matter masses away from one-half the Higgs boson mass, $m_h/2$, either heavier or lighter, there is no such resonance annihilation and thus the Higgs boson-dark matter coupling κ must be fairly large, $\kappa > \mathcal{O}(0.1)$, or else the dark matter would decouple at a sufficiently early stage in the evolution of the universe so that there would be more dark matter present today than what is observed. Thus for most values of m_S (m_S greater than or less than $m_h/2$), the dark matter abundance calculation favors a higher value of $\kappa(>\mathcal{O}(0.1))$.

In this paper, we study the quantum effects of dark matter as modeled by this standard model singlet scalar on the Higgs-inflaton effective potential. As a result of the coupling of the Higgs boson and dark matter singlet, the cosmological restrictions which include up to 3 standard deviations from the measured central values, allow for lower values of the Higgs boson mass than is the case in the absence of such dark matter couplings. In Sec. II, the renormalization group improved effective potential for the physical Higgs field is determined including the effects of its coupling to the scalar singlet dark matter as well as its large nonminimal coupling to the gravitational Ricci sca-

[*]clark@physics.purdue.edu
[†]liu115@physics.purdue.edu
[‡]love@physics.purdue.edu
[§]terveldhuis@macalester.edu

lar. Three quantities, ϵ, η, and ζ^2, parametrizing slow roll inflation are given in terms of the derivatives of this Higgs-inflaton effective potential. The Higgs nonminimal coupling ξ to gravity is specified at the onset of inflation so as to yield the measured value for the amplitude of density perturbations. The scale for the onset of slow roll inflation is set so as to provide $N_e = 60$ e-folds of expansion before the inflaton exits inflation at $\epsilon = 1$. The spectral index, its running, and the tensor to scalar ratio are then determined quantities which depend on the Higgs boson mass as well as the Higgs boson-dark matter coupling and the singlet self-coupling. The numerical results for this dependence are presented in Sec. III and are displayed in Figs. 5 and 8 in terms of cosmologically allowed and excluded regions of parameter space. Conclusions are summarized in Sec. IV. Appendix A provides the one-loop renormalization group β functions for the gravitationally nonminimally coupled model. Appendix B contains the triviality and vacuum stability constraints for the scalar coupling constants.

II. HIGGS-INFLATON EFFECTIVE POTENTIAL

A minimal way of accounting for the presence of non-baryonic dark matter is by modeling said matter by a stable Hermitian standard model singlet, scalar field S. The stability of this scalar is guaranteed through the imposition of an unbroken Z_2 discrete symmetry under which the scalar is odd. Focusing on the scalar and gravitational sector of this model the tree level action in the Jordan frame including all terms through mass dimension four is specified by

$$\Gamma_{\text{Tree}} = \int d^4x \sqrt{-g}\Big[\Lambda + \frac{1}{2}m_{\text{Pl}}^2 R + (D_\mu H)^\dagger g^{\mu\nu}D_\nu H$$
$$- V(H^\dagger H) + \xi R\Big(H^\dagger H - \frac{v^2}{2}\Big) + \frac{1}{2}\partial_\mu S g^{\mu\nu}\partial_\nu S$$
$$- \frac{1}{2}m_S^2 S^2 - \frac{\lambda_S}{4}S^4 + \frac{1}{2}\xi_S R S^2 - \kappa S^2\Big(H^\dagger H - \frac{v^2}{2}\Big)$$
$$+ \cdots\Big] \tag{1}$$

where the Higgs potential is

$$V(H^\dagger H) = \lambda\Big(H^\dagger H - \frac{v^2}{2}\Big)^2 \tag{2}$$

with the Higgs multiplet parametrized by

$$H = \frac{1}{\sqrt{2}}\begin{pmatrix} \chi^+ \\ (v+h) + \chi^0 \end{pmatrix}. \tag{3}$$

Here $\chi^\pm$, χ^0 are the standard model erstwhile Nambu-Goldstone bosons and h the physical Higgs boson field. The ellipses in Eq. (1) refer to the usual remaining standard model Yang-Mills and fermion kinetic terms and Yukawa couplings. Note that this action includes the nonminimal

coupling of the Higgs doublet to the gravitational Ricci scalar R with coupling ξ. m_{Pl}^2 is the reduced Planck mass $m_{\text{Pl}}^2 = 1/8\pi G \approx (2.43 \times 10^{18})^2 \text{ GeV}^2$ and $v = 246.2$ GeV is the scale of electroweak symmetry breaking.

The various cosmological parameters governing the slow roll inflation are secured in terms of derivatives of the effective potential with respect to the Higgs-inflaton field evaluated during the inflationary phase when (only) the physical Higgs field has a large expectation value, $h \sim m_{\text{Pl}}/\sqrt{\xi} \gg v$. Thus it is necessary to determine the renormalization group improved effective potential as a function of h. The nonminimal gravitational interaction of the Higgs doublet couples the gravitational and Higgs fields' equations of motion. This results in a modified form for the high energy behavior of the Higgs and gravitational field propagators or, in the external gravitational field case focused on here, a modified Higgs propagator [14]. At the tree level, the nonminimal Einstein equations obtained from (1) are

$$\Big(1 + \frac{\xi h^2}{m_{\text{Pl}}^2}\Big)\Big(R_{\mu\nu} - \frac{1}{2}R g_{\mu\nu}\Big) = -\frac{1}{m_{\text{Pl}}^2}(\Theta_{\mu\nu} + S_{\mu\nu}), \quad (4)$$

where the new, improved energy-momentum tensor is $\Theta_{\mu\nu} = T_{\mu\nu} + \xi(\frac{1}{2}(\nabla_\mu\nabla_\nu + \nabla_\nu\nabla_\mu) - g_{\mu\nu}\nabla^2)h^2$ with $T_{\mu\nu}$ the standard model canonical energy-momentum tensor. $S_{\mu\nu}$ are terms involving the dark matter field S and its coupling to itself, the gravitational field, and the standard model Higgs field. Focusing on the gravitational and Higgs fields only as they are dominant in the inflationary region, the trace of Eq. (4) results in

$$\Big(1 + \frac{\xi h^2}{m_{\text{Pl}}^2}\Big)R = \frac{-1}{m_{\text{Pl}}^2}\Big(6\xi h\nabla^2 h + 6\Big(\xi + \frac{1}{6}\Big)\nabla h \cdot \nabla h$$
$$- 4V(h)\Big). \tag{5}$$

Substituting this into the Higgs field equation yields

$$\nabla^2 h + V'(h) = \xi h R$$
$$= \frac{-6\xi^2 h^2/m_{\text{Pl}}^2}{(1 + \xi h^2/m_{\text{Pl}}^2)}\nabla^2 h$$
$$- \frac{\xi h(6(\xi + 1/6)\nabla h \cdot \nabla h - 4V(h))}{(m_{\text{Pl}}^2 + \xi h^2)}. \tag{6}$$

Expanding about the background Higgs field $h \to h + \rho$, produces the field equation

$$\frac{1}{s(h)}\nabla^2\rho = -V' + \cdots, \tag{7}$$

where (primes denote differentiation with respect to h)

$$s(h) = \frac{1 + \xi h^2/m_{\text{Pl}}^2}{1 + (1 + 6\xi)\xi h^2/m_{\text{Pl}}^2}. \tag{8}$$

Thus the nonminimal coupling to the gravitational field introduces a modification to the Higgs field propagator by a factor of $s(h)$. The one-loop renormalization group improved effective potential for h can now be computed using standard techniques. The only modification to the standard model calculation arises from the noncanonical Higgs kinetic term. Thus for large nonminimal gravitational coupling constants, ξ, and for the sizeable, but still sub-Planckian, inflationary backgrounds $h \sim m_{Pl}/\sqrt{\xi}$, this leads to a suppression of the physical Higgs field propagator [4,12,14]

$$i/p^2 \rightarrow is/p^2. \tag{9}$$

Note that $s(h)$ takes its canonical value $s(h) \rightarrow 1$ when $\frac{\xi h^2}{m_{Pl}^2} \ll 1$ while in the other extreme, $s(h) \rightarrow \frac{1}{6\xi}$ when $\frac{\xi h^2}{m_{Pl}^2} \gg 1$.

It then follows, for these large field values, the Higgs field is no longer an unconstrained high energy degree of freedom. This will result in a violation of unitarity and an (as yet unknown) ultraviolet completion of the model will be necessary for a thorough understanding of the dynamics in the inflationary region [26]. Moreover, although h is sub-Planckian in the inflationary region, the variable $\sqrt{\xi}h/m_{Pl}$ is large and the issue of contributions from higher dimensional operators needs further scrutiny. As discussed in Ref. [13], the Higgs suppression could indicate the onset of a new strongly interacting phase of the Higgs sector of the standard model. To account for this, the perturbative low energy standard model renormalization group running of the coupling constants was matched onto their running in a nonlinearly realized electroweak symmetry model effective in the range $m_{Pl}/\xi < h < m_{Pl}/\sqrt{\xi}$ where the Higgs field contributions to processes are absent [13]. Here we adopt a somewhat pragmatic approach and following in the spirit of Ref. [12], we employ the suppressed Higgs effective standard model, now with the inclusion of the dark matter scalar, and explore the dependence of the measured cosmological density spectrum parameters on the Higgs and dark matter coupling constants for the inflationary scales $h \sim m_{Pl}/\sqrt{\xi}$, albeit possibly at the limits of its domain of validity. Hence, Feynman integrands involving Higgs propagators will have a suppression factor s for each such line with $s(h)$ evaluated at the scale of the background Higgs field h. In particular the renormalization group functions will include a suppression factor for each physical Higgs line contributing to the function.

Isolating the explicit dependence on the dominant large Higgs field background terms, while the ellipses refer to the remaining subdominant singlet and standard model terms, the one-loop renormalization group improved effective action takes the form

$$\Gamma = \int d^4x \sqrt{-g} \left[\Lambda + \frac{1}{2}m_{Pl}^2 f(t)R + \frac{1}{2}G^2(t)\partial_\mu h g^{\mu\nu}\partial_\nu h \right.$$
$$\left. - V(t) + \cdots \right]. \tag{10}$$

In the inflationary region, the Higgs-inflaton field has a large background value and the dominant forms of the renormalization group improved effective action coefficients are

$$V(t) = \frac{\lambda(t)}{4}G^4(t)h^4(t) = \frac{\lambda(t)}{4}G^4(t)m_t^4 e^{4t} \tag{11}$$

$$f(t) = 1 + \xi(t)G^2(t)\frac{h^2(t)}{m_{Pl}^2} = 1 + \xi(t)G^2(t)\frac{m_t^2}{m_{Pl}^2}e^{2t},$$

where

$$G(t) = e^{-\int_0^t dt' \gamma(t')}, \tag{12}$$

with $\gamma(t)$ the Higgs field anomalous dimension. Here we have introduced the scaling variable $t = t(h) = \ln(h/m_t)$ so that $h(t) = m_t e^t$ and have normalized the Higgs field and all running couplings at the top quark mass. The various t dependent running coupling constants of the effective interaction terms are given by their renormalization group equations so that, for example,

$$\frac{d\lambda(t)}{dt} = \beta_\lambda(t), \qquad \frac{d\xi(t)}{dt} = \beta_\xi(t). \tag{13}$$

The one-loop β functions and Higgs field anomalous dimension including the suppression factors are compiled in Appendix A.

Cosmological quantities can most readily be calculated in the Einstein frame which is obtained by rescaling the metric by $g_{E\mu\nu} = f(t)g_{\mu\nu}$. The one-loop renormalization group improved effective action then takes the form

$$\Gamma = \int d^4x \sqrt{-g_E} \left[\Lambda_E + \frac{1}{2}m_{Pl}^2 R_E \right.$$
$$\left. + \frac{1}{2}\frac{1}{f(t)\bar{s}(t)}\partial_\mu h g_E^{\mu\nu}\partial_\nu h - V(t)/f(t)^2 + \cdots \right], \tag{14}$$

where

$$\bar{s}(t) = \frac{f(t)}{G^2(t)f(t) + \frac{3}{2}m_{Pl}^2 f'^2(t)}. \tag{15}$$

Defining a canonically normalized field $\sigma = \sigma(h)$, the Einstein frame effective action reads

$$\Gamma = \int d^4x \sqrt{-g_E} \left[\Lambda_E + \frac{1}{2}m_{Pl}^2 R_E + \frac{1}{2}\partial_\mu \sigma g_E^{\mu\nu}\partial_\nu \sigma \right.$$
$$\left. - V_E(\sigma) + \cdots \right], \tag{16}$$

where the dominant part of the one-loop renormalization group improved effective potential in the inflationary region in the Einstein frame is

$$V_E = \frac{V(t)}{f^2(t)} \qquad (17)$$

with the canonically normalized Higgs-inflaton field defined through

$$\left(\frac{d\sigma}{dh}\right)^2 = \frac{1}{f\bar{s}} = \frac{G^2 f + \frac{3}{2}m_{\rm Pl}^2 f'^2}{f^2}. \qquad (18)$$

A Higgs field wave function renormalization suppression factor is now defined as

$$Z(t) \equiv G^2(t)\bar{s}(t) = \frac{G^2(t)f}{G^2(t)f + \frac{3}{2}m_{\rm Pl}^2 f'^2}$$

$$= \frac{1 + \psi^2(t)}{(1 + [1 + 6\xi(t)(1 - \gamma(t) + \beta_\xi/2\xi(t))^2]\psi^2(t))}, \qquad (19)$$

where

$$\psi^2(t) = \xi(t)G^2(t)h^2(t)/m_{\rm Pl}^2 = \xi(t)G^2(t)e^{2t}m_t^2/m_{\rm Pl}^2 \quad (20)$$

is a renormalization group invariant dimensionless field. Note that $f(t) = 1 + \psi^2(t)$. As a function of $\psi(t)$, the Higgs-inflaton effective potential takes the simple form

$$V_E = \frac{m_{\rm Pl}^4}{4} \frac{\lambda(t)}{\xi^2(t)} \frac{\psi^4(t)}{(1 + \psi^2(t))^2}. \qquad (21)$$

The renormalization group invariant slow roll inflationary parameters are defined by (once again prime denotes differentiation with respect to h)

$$\epsilon = \frac{1}{2}m_{\rm Pl}^2 \left(\frac{1}{V_E}\frac{dV_E}{d\sigma}\right)^2 = \frac{1}{2}m_{\rm Pl}^2 \left(\frac{V_E'}{V_E}\right)^2 \left(\frac{d\sigma}{dh}\right)^{-2}$$

$$= 8\xi \frac{Z}{f\psi^2}\left(1 - \gamma + \frac{\beta_\lambda}{4\lambda} + \psi^2\left(\frac{\beta_\lambda}{4\lambda} - \frac{\beta_\xi}{2\xi}\right)\right)^2$$

$$\eta = m_{\rm Pl}^2 \frac{1}{V_E}\frac{d^2 V_E}{d\sigma^2} = 2\epsilon + m_{\rm Pl}\frac{1}{\sqrt{2\epsilon}}\frac{d\epsilon}{dh}\left(\frac{d\sigma}{dh}\right)^{-1}$$

$$= 2\epsilon + \frac{\sqrt{\xi f Z}}{\sqrt{2\epsilon}}\left(\frac{1}{\psi}\right)\frac{d\epsilon}{dt}$$

$$\zeta^2 = m_{\rm Pl}^4 \frac{1}{V_E}\frac{d^3 V_E}{d\sigma^3}\frac{1}{V_E}\frac{dV_E}{d\sigma} = 2\eta\epsilon + m_{\rm Pl}\sqrt{2\epsilon}\frac{d\eta}{dh}\left(\frac{d\sigma}{dh}\right)^{-1}$$

$$= 2\eta\epsilon + \sqrt{2\epsilon\xi f Z}\left(\frac{1}{\psi}\right)\frac{d\eta}{dt}, \qquad (22)$$

where all quantities are evaluated at the onset of inflation. The power spectrum of density perturbations in k space is given by

$$P_s(k) = \Delta_{\mathcal{R}}^2 \left(\frac{k}{k^*}\right)^{n_s(k)-1}, \qquad (23)$$

where the amplitude of density perturbations is expressed as

$$\Delta_{\mathcal{R}}^2 = \frac{V_E}{24\pi^2 m_{\rm Pl}^4 \epsilon}\bigg|_{k^*} \qquad (24)$$

and is secured by the combination of experimental results from WMAP5, baryon acoustic oscillations, and supernovae as $\Delta_{\mathcal{R}}^2 = (2.445 \pm 0.096) \times 10^{-9}$ at $k^* = 0.002$ Mpc^{-1} [27]. Slow roll inflation predicts the spectral index, n_s, its running, $\alpha = dn_s/d\ln k$, and the tensor to scalar ratio, r, to be

$$n_s = 1 - 6\epsilon + 2\eta \qquad \alpha = -24\epsilon^2 + 16\epsilon\eta - 2\zeta^2$$
$$r = 16\epsilon. \qquad (25)$$

The WMAP5, baryon acoustic oscillations, and supernovae experimental evidence gives $n_s = 0.960 \pm 0.013$ and $r < 0.22$ (95% C.L.) with an insignificant running spectral index, $\alpha = -0.028 \pm 0.020$ [27].

III. NUMERICAL RESULTS

The renormalization group equations for the various running couplings are solved numerically starting from $t = 0$ which corresponds to the top quark mass. The top Yukawa coupling at $t = 0$ is fixed by the central value deduced from the top quark mass $m_t = y_t(0)v/\sqrt{2} \equiv 171.2$ GeV, while the gauge coupling constants are normalized at m_t as $\alpha_1(0) = 0.010\,271\,8$, $\alpha_2(0) = 0.033\,441\,2$, and $\alpha_3(0) = 0.108\,635$ [28]. The value of $\xi(0)$ is determined so that at the initial point of the slow roll inflation, t_i, the nonminimal coupling constant $\xi(t_i)$ is such that the calculated value of the amplitude of density perturbations, Eq. (24), agrees with the measured result. The Higgs-inflaton exits inflation at the final point t_f when the first slow roll parameter is 1: $\epsilon(t_f) = 1$. The number of e-folds of expansion between t_i and t_f is

$$N_e(t_i) = \frac{1}{\sqrt{2}m_{\rm Pl}} \int_{\sigma_f}^{\sigma_i} \frac{d\sigma'}{\sqrt{\epsilon(h(\sigma'))}}$$

$$= \frac{1}{\sqrt{2}m_{\rm Pl}} \int_{h_f}^{h_i} \frac{dh'}{\sqrt{\epsilon(h')}}\left(\frac{d\sigma'}{dh'}\right)$$

$$= \int_{t_f}^{t_i} dt \frac{\psi^2}{4\xi Z}\frac{1}{(1 - \gamma + \frac{\beta_\lambda}{4\lambda} + \psi^2(\frac{\beta_\lambda}{4\lambda} - \frac{\beta_\xi}{2\xi}))}. \quad (26)$$

The initial point of inflation is defined so that $N_e(t_i) = 60$. These three criteria are then implemented recursively for each choice of initial Higgs mass, $m_h = \sqrt{2\lambda(0)}v$ and scalar coupling constants $\kappa(0)$, $\lambda_S(0)$, and $\xi_S(0)$. The standard model without dark matter coupling corresponds to $\kappa(0) = 0 = \lambda_S(0)$.

As evident from Figs. 1 and 2, the shape of the effective potential in the inflation region depends not only on the Higgs boson mass [12–14], but also changes as the Higgs-inflaton to dark matter coupling and dark matter self-coupling varies. The high energy suppression of the Higgs propagator also effects the running of the scalar coupling constants as seen in Figs. 3 and 4. The suppression factor is plotted along with the coupling constants
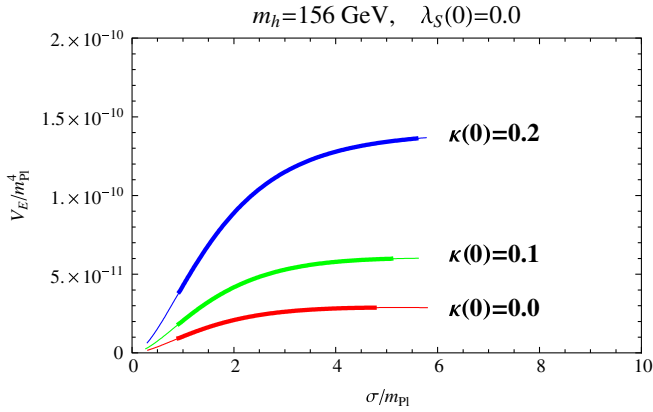
FIG. 1 (color online). The Einstein frame renormalization group improved effective potential as a function of the canonically normalized Higgs-inflaton field. The magnitude and shape of this potential in the inflationary cosmological state varies with the strength of the Higgs-inflaton and dark matter coupling constant κ. The thickened portion of the potential curve corresponds to the $N_e = 60$ e-folds of inflation with onset and exit values of σ as shown.

whose β function dependence on the suppression factor manifests itself in the abrupt change of running.

The fractional rate of change of the effective potential is obtained from the renormalization group equations. Recalling that

$$\frac{d}{dt} \ln \frac{\lambda}{\xi^2} = 4\left(\frac{\beta_\lambda}{4\lambda} - \frac{\beta_\xi}{2\xi}\right)$$

$$\frac{d}{dt} \ln \frac{\psi^4}{(1+\psi^2)^2} = 4\left(\frac{1 - \gamma + \frac{\beta_\xi}{2\xi}}{(1+\psi^2)}\right),$$
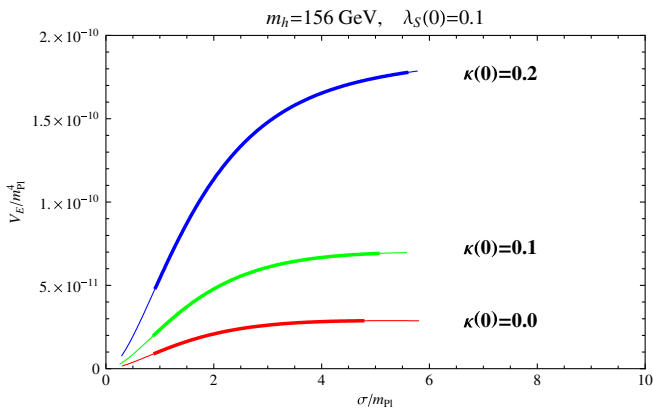(27)

FIG. 2 (color online). The Einstein frame renormalization group improved effective potential as a function of the canonically normalized Higgs-inflaton field. The magnitude and shape of this potential in the inflationary cosmological state varies with the strength of the dark matter self-coupling constant λ_S as compared to Fig. 1 for the different Higgs-inflaton to dark matter coupling κ. The thickened portion of the potential curve corresponds to the $N_e = 60$ e-folds of inflation with onset and exit values of σ as shown.
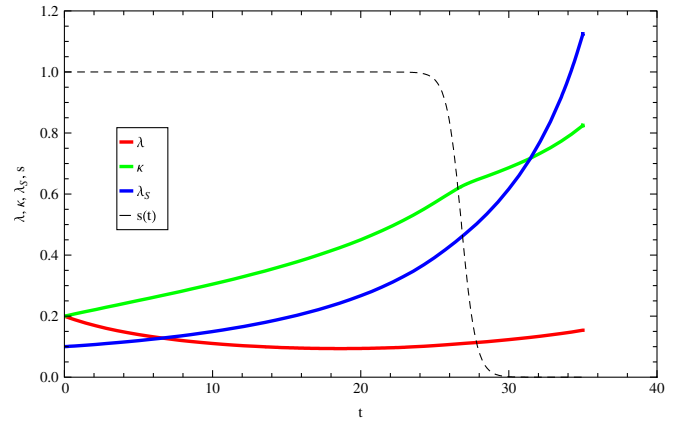

FIG. 3 (color online). The running coupling constants for the scalar fields. The initial conditions for the coupling constants correspond to the effective potential plot of Fig. 2 with $\kappa(0) = 0.2$, $\xi(0) = 8,315$, and $\xi_S(0) = 0.0$. In this case the onset of inflation occurred at the scale $t_i = 35$ with exit at $t_f = 32.7$ after 60 e-folds of expansion.

it follows that

$$\frac{d}{dt} \ln V_E = \frac{4}{(1+\psi^2)}\left(1 - \gamma + \frac{\beta_\lambda}{4\lambda} + \psi^2\left[\frac{\beta_\lambda}{4\lambda} - \frac{\beta_\xi}{2\xi}\right]\right).$$
(28)

For larger values of $\lambda(0)$ and hence more massive Higgs bosons, the term in the square bracket can cancel the remaining bracketed terms since $\psi^2\beta_\xi/2\xi$ is getting large. Thus there will be some t value at which the effective potential reaches a maximum value, the wrong way roll point, before turning over and decreasing as the scale is increased. For a Higgs-inflaton model to be viable, it is thus necessary that the inflation must initiate at t_i values less than that of this relative maximum or else the inflaton rolls
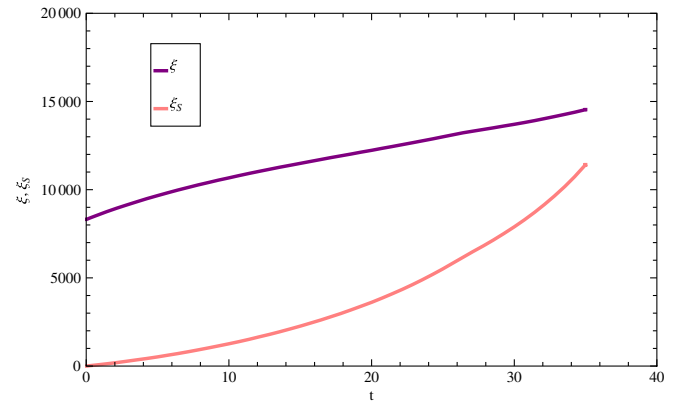

FIG. 4 (color online). The running of the nonminimal gravitational coupling constants for the scalar fields. The initial conditions for the coupling constants correspond to the effective potential plot of Fig. 2 with $\kappa(0) = 0.2$, $\xi(0) = 8,315$, and $\xi_S(0) = 0.0$. In this case the onset of inflation occurred at the scale $t_i = 35$ with exit at $t_f = 32.7$ after 60 e-folds of expansion.

to $m_{\rm Pl}$ and beyond. The scale at which this cannot be accomplished sets an upper limit on the Higgs mass consistent with the inflationary cosmology model. It is typically below that of the suppressed triviality bound which is mapped out in Appendix B. Hence, an additional region of parameter space previously allowed by the suppressed triviality constraint, as seen in Fig. 10, will be ruled out due to the wrong way roll condition. Likewise, for smaller values of $\lambda(0)$ that lead to a running close to the vacuum stability bound, β_λ/λ is negatively large enough so that a relative maximum forms in the effective potential. Thus once again, there is a region of parameter space not ruled out by vacuum stability but excluded by the wrong way roll

condition. Moreover, since the effective potential has a maximum before vacuum instability and the onset of inflation are reached, the wrong way roll excluded area covers that previously ascribed to vacuum instability. The wrong way roll criterion more severely restricts the parameter space of the model than the requirement of absolute vacuum stability up to the onset of inflation. For that matter, even if the absolute stability constraint is abandoned in favor of vacuum metastability [29] with a lifetime longer than the age of the observable universe, then the additional range of Higgs boson masses allowed by this less stringent condition are ruled out by the imposition of the wrong way roll constraint. Hence for both low and high
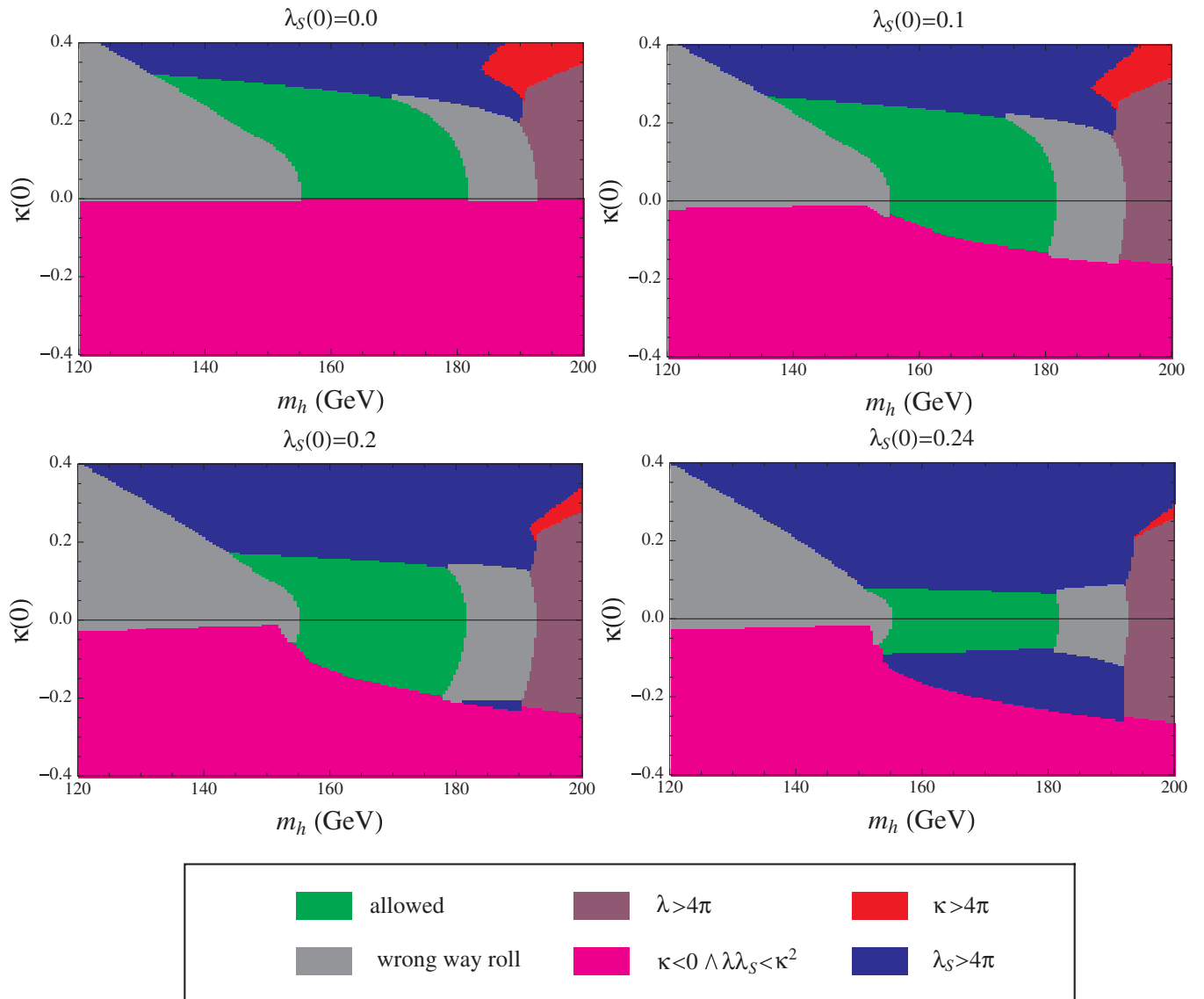

FIG. 5 (color online). The wrong way roll constraints for parameter space are added to those of vacuum stability and triviality (compare to Fig. 10). These are displayed for typical initial nonminimal gravitational couplings of $\xi(0) = 10^4$ and $\xi_S(0) = 0.0$. The grey colored areas mark the wrong way roll excluded regions of parameter space. The constraints apply to scales up to those typical of the onset of inflation, $t_i = 34.5$.

Higgs masses, additional regions of parameter space are excluded as they do not support slow roll inflation. For typical values of the scalar parameters the wrong way roll excluded region of parameter space is displayed in Fig. 5.

For $\kappa(0) = \lambda_S(0) = 0$, the allowed range of Higgs boson masses after the imposition of the wrong way roll constraint is roughly 155 GeV $< m_h <$ 182 GeV. This is a slightly smaller range than that allowed without the additional constraint which is 153 GeV $< m_h <$ 190 GeV (see Appendix B). Still considering $\lambda_S(0) = 0$, as $\kappa(0)$ increases, the smallest allowed m_h value consistent with the various constraints is approximately 130 GeV, which is roughly the same as without the wrong way roll constraint. This occurs when $\kappa(0) \simeq 0.3$. For larger values of $\kappa(0)$, the allowed parameter space vanishes. Once again, this is akin to the case without the wrong way roll constraint. As $\lambda_S(0)$ increases from zero, the allowed parameter space starts to shrink as a smaller range of $\kappa(0)$ values are permitted, while there remains a finite range of allowed Higgs boson masses. Finally, for $\lambda_S(0) > 0.25$, the allowed

$\kappa(0)$ range vanishes for a finite range of allowed Higgs boson masses. Hence the allowed parameter space disappears. While Fig. 5 corresponds to particular value of $\xi(0)$, the generic features continue to hold for a range of large $\xi(0)$ values.

The viable region of parameter space is further restricted by the requirement of yielding a value of the spectral index within its experimentally determined range. Once the effective potential is determined, the cosmological quantities are calculated using Eqs. (22) and (25). The spectral index, its running, and the tensor to scalar ratio are plotted versus the Higgs boson mass in Figs. 6 and 7 for various initial values of the Higgs-inflaton to dark matter coupling and for two initial values of the dark matter self-coupling. The green area shown in Fig. 8 corresponds to model values of n_s that are within 1 standard deviation of the experimental central value for the spectral index, $n_s = 0.960$ [27]. The yellow area is determined by the predicted value of n_s being between 1 and 2 standard deviations of its central value. The orange regions correspond to n_s predicted val-
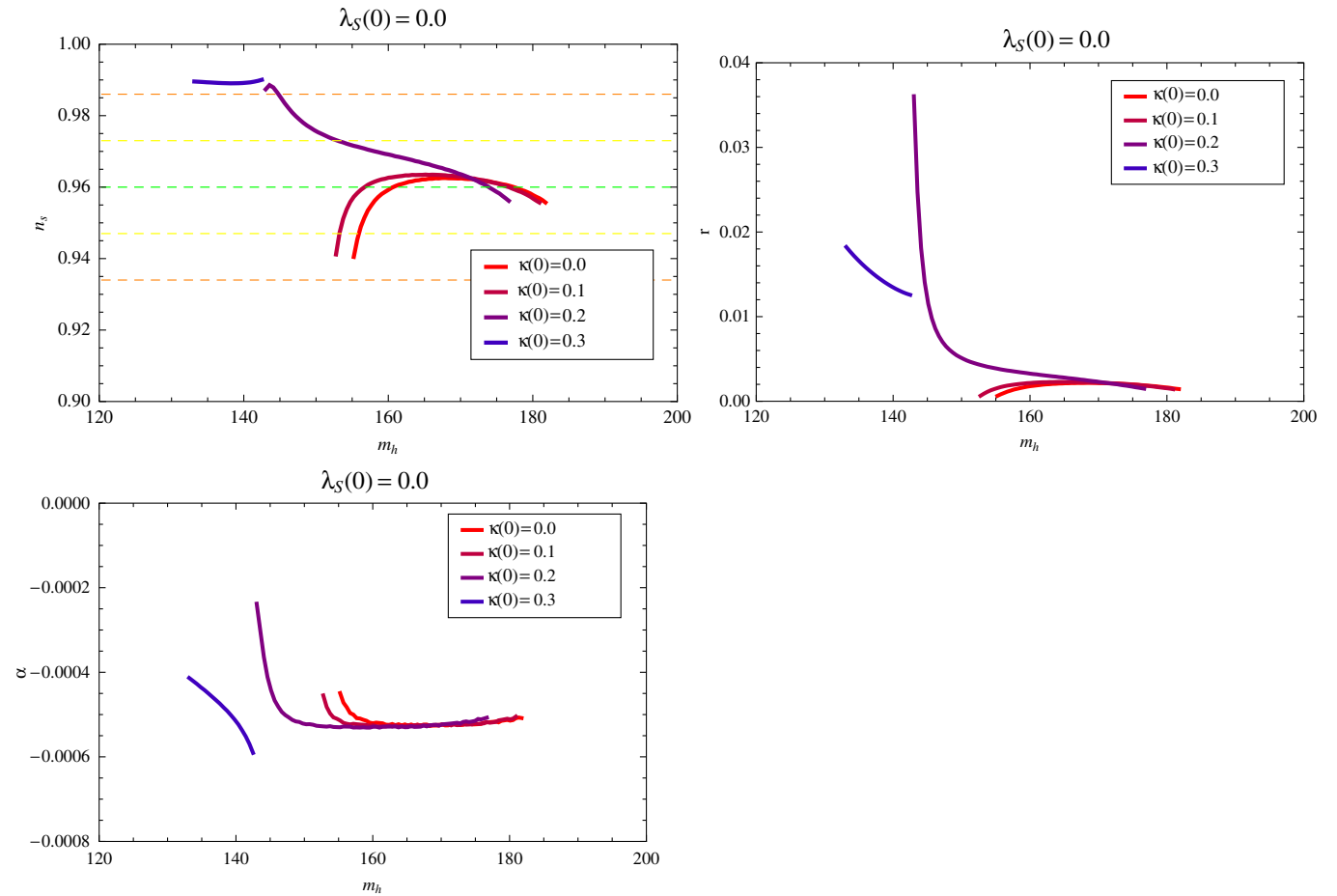

FIG. 6 (color online). The spectral index n_s, its running α and the tensor to scalar ratio r are plotted against the Higgs mass m_h for various values of the Higgs-inflaton to dark matter coupling constant $\kappa(0)$ for the fixed initial value of the dark matter self-coupling $\lambda_S(0) = 0.0$. Curve endpoints are determined by the wrong way roll, triviality, and vacuum stability conditions. The dashed horizontal lines in the spectral index plot denote its central value, 0.960, and 1 and 2 standard deviations from it.
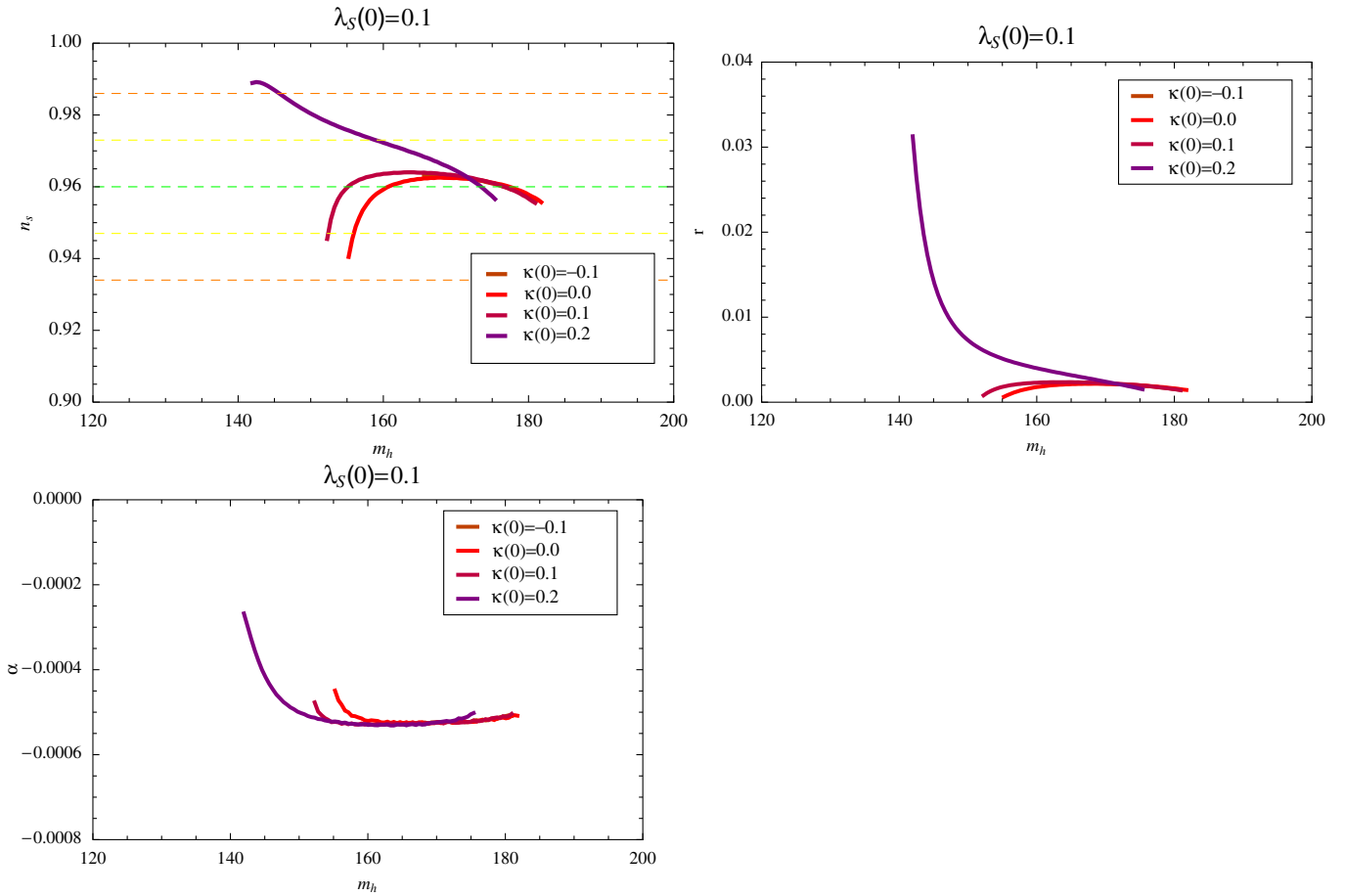
FIG. 7 (color online). The spectral index n_s, its running α, and the tensor to scalar ratio r are plotted against the Higgs mass m_h for various values of the Higgs-inflaton to dark matter coupling constant $\kappa(0)$ for the fixed initial value of the dark matter self-coupling $\lambda_S(0) = 0.1$. Curve endpoints are determined by the wrong way roll, triviality, and vacuum stability conditions. The dashed horizontal lines in the spectral index plot denote its central value, 0.960, and 1 and 2 standard deviations from it. Note that the curves corresponding to $\kappa(0) = -0.1$ and $\kappa(0) = 0.0$ cannot be distinguished up to the thickness of the lines.

ues to be within 2 to 3 standard deviations from the central value. Finally the red regions indicate a predicted spectral index greater than 3 standard deviations beyond the central value. The grey regions are excluded by triviality, vacuum stability, and the wrong way roll conditions.

In general, as the Higgs boson to dark matter coupling strength, $\kappa(0)$, increases, lower values of the Higgs mass will still support a stable vacuum as well as avoid the wrong way roll condition. However, a tension begins to arise between the experimentally allowed values of the spectral index and the model values of the index at low Higgs mass. It follows from Figs. 6–8 that, consistent with the triviality, vacuum stability, and wrong way roll constraints, agreement with the central measured value of n_s favors a Higgs boson mass in the range 155–180 GeV and a smaller value of $\kappa(0)$. As $\kappa(0)$ grows to values $\simeq 0.3$, the computed value of n_s lies between 1 to 3 standard deviations above the central measured value and occurs for smaller Higgs boson masses of order 130–145 GeV. Thus

a discovery of a Higgs boson mass in this range favors both a larger spectral index and a larger coupling to dark matter as is also preferred by the dark matter abundance calculations provided the dark matter is either lighter or heavier than $\sim m_h/2$. Note that there is no additional constraint arising from r and α as their computed values lie well below the present experimental limits.

As noted previously, the parameter space available shrinks as the dark matter self-coupling increases as displayed in Fig. 8 for different $\lambda_S(0)$ slices. This self-coupling is largely unconstrained by dark matter experiments and observations. For small dark matter mass (less than ~ 1 GeV) a correlation between the self-coupling and mass may soften current discrepancies between the observed dark matter halo structure and numerical simulations of the structure formation process [30,31]. Overall there is ample parameter space available for a consistent minimal standard model with the Higgs boson acting as the inflaton and interacting with scalar dark matter.
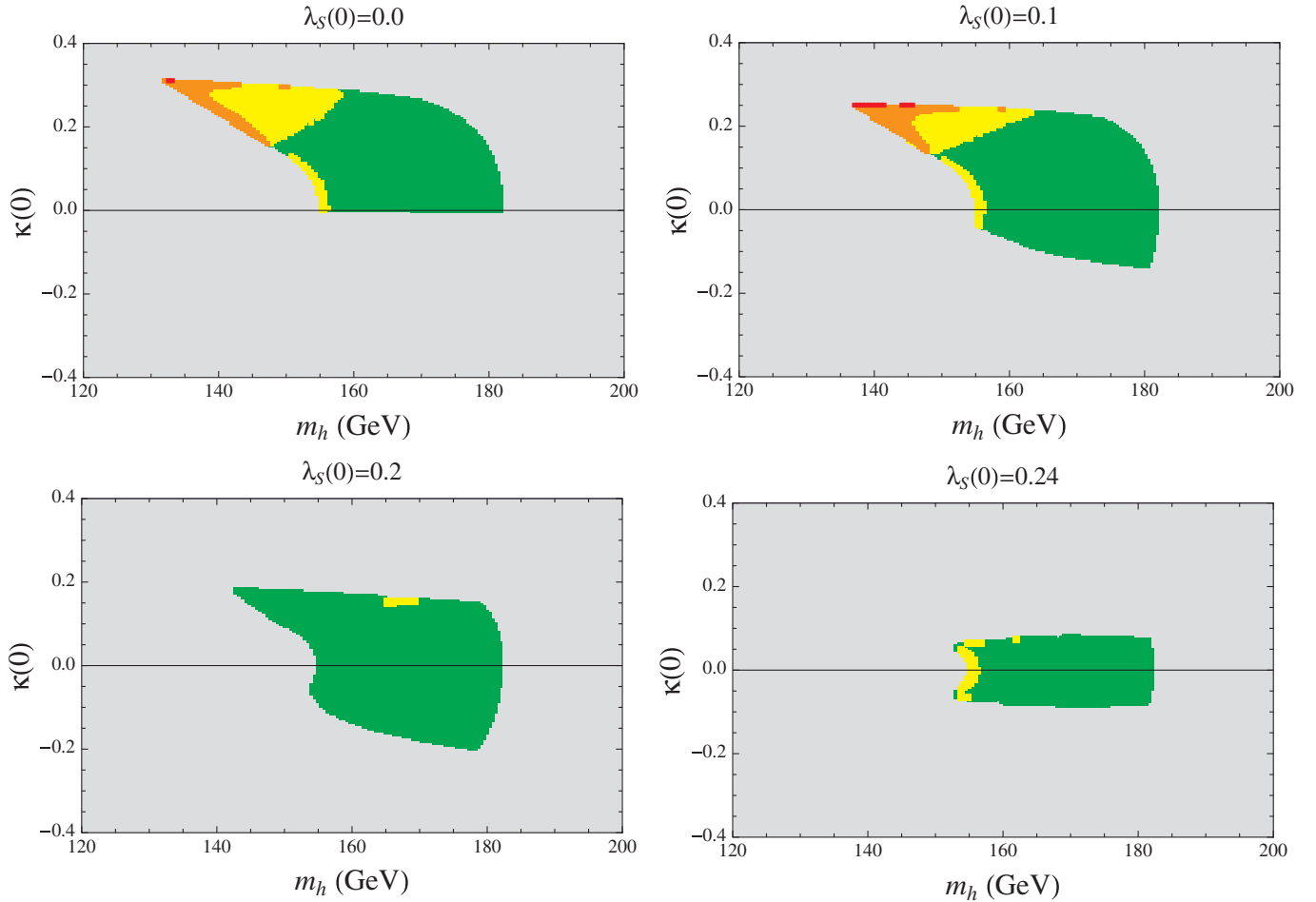
FIG. 8 (color online).   The spectral index cosmological constraints on slices of parameter space for different dark matter self-coupling λ_S as determined by the degree of agreement with the experimental value of the spectral index, $n_s = 0.960$. These constraints are applied to the potentially allowed (green) areas displayed in Fig. 5. Here the green regions indicate the volume of parameter space that predicts spectral index values within 1 standard deviation of the central value. The yellow regions correspond to calculated values between 1 and 2 standard deviations of the central value, while the orange regions correspond to 2 to 3 standard deviations from it. The red areas indicate parameters that predict spectral index values more than 3 standard deviations from the central value. Finally the grey region is excluded by triviality and vacuum stability bounds along with the wrong way roll condition. For $\lambda_S(0) \geq 0.25$, there is no allowed region of parameter space.

IV. CONCLUSIONS

The influence of the inclusion of dark matter on slow roll inflation models where the inflaton is identified with the standard model Higgs boson was explored. To achieve this, the standard model was modified by the inclusion of an Hermitian scalar standard model singlet field, which accounts for the observed abundance of dark matter and the lack of its direct detection, and a large nonminimal coupling of the Higgs doublet to the Ricci scalar curvature. The model parameter space thus included the Higgs boson and singlet scalar masses, the scalar self-coupling and the coupling between the Higgs doublet and the dark matter in addition to the nonminimal gravitational couplings of both the Higgs doublet and the singlet scalar. In the inflationary region where the physical Higgs field develops a sizeable classical background, the presence of the large Higgs doublet nonminimal gravitational coupling results in a highly suppressed physical Higgs field propagator. Accounting for this, the one-loop renormalization group improved effective potential was computed and the constraints on the model parameter space were delineated. In addition to the usual triviality and vacuum stability bounds, we focused on the cosmological constraints arising from the identification of the Higgs boson with the inflaton. Since, in general, the one-loop effective potential develops a maximum, it was necessary to insure that the onset of inflation occurred such that the inflaton rolling was toward the origin and not towards the Planck scale. The implication of this wrong way roll constraint is displayed in Fig. 5 and is seen to eliminate even more of the parameter space than the vacuum stability (or metastability) constraint.

Various parameters characterizing the slow roll inflation were computed with the spectral index, n_s, providing the most stringent constraint on the coupling constant space. As is seen in Fig. 8, the region of parameter space allowed after the imposition of wrong way roll, triviality, and vacuum stability constraints, is further partitioned into various sections whose agreement with the measured spectral index is only at a varying number (1–3) of standard deviations above the central value. Larger values of the coupling of the Higgs-inflaton to dark matter, as is preferred by the dark matter abundance calculation, lead to a lower allowed range of Higgs boson masses. In addition, there are the various Higgs mass bounds from accelerator experiments. The direct LEP search [32] gives a lower bound of 114.4 GeV, while a fit to electroweak precision data prefers [33] a mass $m_h < 182$ GeV. Finally, a combined CDF and DO analysis of Tevatron data [34] excludes the range 160 GeV $< m_h <$ 170 GeV. While our analysis has been limited to the one-loop radiative corrections, we anticipate that the general features of our results will continue to hold when two and higher loop corrections are included. Thus there will be a range of lower allowed Higgs boson masses with increasing Higgs boson-dark matter coupling. Moreover, we expect that the changes to the wrong way roll constraint arising from the inclusion of two-loop effects will restrict the parameter space in an analogous fashion to the two-loop changes in the vacuum stability and triviality bounds. For the model in the absence of any dark matter ($\kappa(0) = \lambda_S(0) = 0$), the two-loop result yields a larger allowed range of Higgs boson masses than does the one-loop result [13]. Thus we conclude that even after the inclusion of the dark matter, there still remains a range of LHC attainable Higgs boson mass values that are consistent with the cosmological parameters of slow roll inflation when the Higgs scalar is identified as the inflaton.

APPENDIX A: RENORMALIZATION GROUP EFFECTIVE COUPLING CONSTANTS

To secure the one-loop renormalization group β functions including the Higgs field suppression factors, we employed the analysis of [35]. Isolating those graphs containing a physical Higgs field propagator, we included a suppression factor $s(t)$ for each such line. In addition, the various combinatorial factors were appropriately modified. No suppression factors were included for the erstwhile Nambu-Goldstone fields nor any other propagators

[19,36]. So doing, we find

$$(4\pi)^2 \frac{dg_1}{dt} = g_1^3 \left(\frac{81 + s(t)}{12} \right)$$

$$(4\pi)^2 \frac{dg_2}{dt} = -g_2^3 \left(\frac{39 - s(t)}{12} \right)$$

$$(4\pi)^2 \frac{dg_3}{dt} = -7 g_3^3$$

$$(4\pi)^2 \frac{dy_t}{dt} = y_t \left(\left(\frac{23}{6} + \frac{2}{3} s(t) \right) y_t^2 - 8 g_3^2 - \frac{17}{12} g_1^2 - \frac{9}{4} g_2^2 \right)$$

$$(4\pi)^2 \frac{d\lambda}{dt} = \Bigg((6 + 18 s^2(t)) \lambda^2 - 6 y_t^4$$
$$+ \frac{3}{8} (2 g_2^4 + (g_1^2 + g_2^2)^2) + 12 y_t^2 \lambda - 3 g_1^2 \lambda$$
$$- 9 g_2^2 \lambda + 2 \kappa^2 \Bigg)$$

$$(4\pi)^2 \frac{d\kappa}{dt} = \kappa \Bigg(8 s(t) \kappa + 6(1 + s^2(t)) \lambda + 6 \lambda_S + 6 y_t^2$$
$$- \frac{3}{2} g_1^2 - \frac{9}{2} g_2^2 \Bigg)$$

$$(4\pi)^2 \frac{d\lambda_S}{dt} = 18 \lambda_S^2 + (6 + 2 s^2(t)) \kappa^2$$

$$(4\pi)^2 \frac{d\xi}{dt} = \left(\xi + \frac{1}{6} \right) \left(6(1 + s^2(t)) \lambda + 6 y_t^2 - \frac{3}{2} g_1^2 - \frac{9}{2} g_2^2 \right)$$
$$+ \left(\xi_S + \frac{1}{6} \right) 2 \kappa$$

$$(4\pi)^2 \frac{d\xi_S}{dt} = \left(\xi_S + \frac{1}{6} \right) 6 \lambda_S + \left(\xi + \frac{1}{6} \right) (6 + 2 s^2(t)) \kappa. \quad \text{(A1)}$$

The Higgs field propagator suppression factor in the inflationary background, where $h(t) = m_t e^t$, is given by

$$s(t) = \frac{1 + \xi(t) m_t^2 e^{2t}/m_{\text{Pl}}^2}{1 + (1 + 6\xi(t))\xi(t) m_t^2 e^{2t}/m_{\text{Pl}}^2} \quad \text{(A2)}$$

and the Higgs field one-loop anomalous dimension γ is (in Landau gauge)

$$(4\pi)^2 \gamma = 3 y_t^2 - \frac{3}{4} g_1^2 - \frac{9}{4} g_2^2. \quad \text{(A3)}$$

The suppression factors in these renormalization group equations differ somewhat from those inserted in the one-loop terms of the beta functions presented in Ref. [12]. The resulting differences in numerical values are small. Our results also differ from those obtained by Ref. [13]. The origin of this difference is discussed in Sec. II.

APPENDIX B: TRIVIALITY AND VACUUM STABILITY

The effective coupling constants can be determined by integrating the one-loop renormalization group equations detailed in Appendix A. The constraints due to absolute vacuum stability of the scalar sector provide lower bounds

on the initial values of the coupling constants. Vacuum stability requires that $\lambda \geq 0$, $\lambda_S \geq 0$ and for $\kappa < 0$ the relation $\lambda \lambda_S \geq \kappa^2$ must hold for all values of t in the range of applicability of the effective theory. For the theory to remain in the perturbative sector of the model, the scalar coupling constants must not reach their respective Landau singularities for all values of t in the range of applicability of the effective theory. Thus we require the so-called triviality bounds that the coupling constants to be less than 4π, $\lambda < 4\pi$, $\lambda_S < 4\pi$, and $\kappa < 4\pi$.

In the following two sets of figures, the allowed parameter space, after the imposition of these vacuum stability and triviality constraints, is mapped out as a function of the various $t = 0$ couplings ($m_h = \sqrt{2\lambda(0)}v$). The triviality or

vacuum stability bound that is violated for the various regions of the parameter space is indicated. In Fig. 9, the parameter space constraints are applicable up to $t = 38$ which corresponds to a scale slightly larger than the reduced Planck mass and with no suppression of the Higgs propagator [$s(t) = 1$].

A two-loop analysis of the vacuum stability and triviality bounds on the Higgs boson mass in the standard model without the singlet scalar was performed in Refs. [37]. The adoption of two-loop beta functions in conjunction with implementation of one-loop Higgs and top quark pole-mass definitions in those studies is seen to lower the lower limit on the physical Higgs boson mass by about 25 GeV
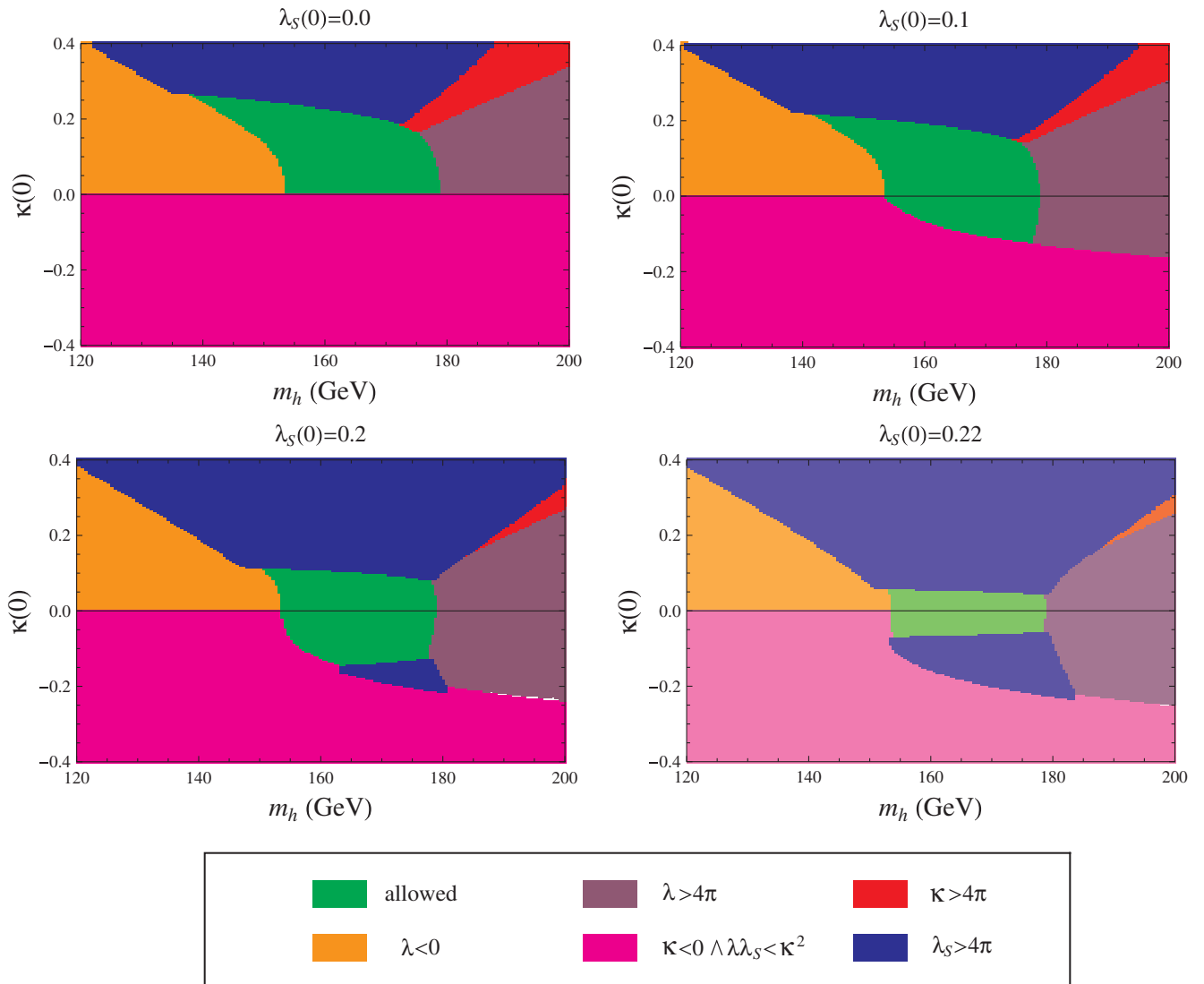

FIG. 9 (color online). The vacuum stability and triviality constraints are applied to the parameter space [i.e. $\lambda(0)$, $\kappa(0)$, $\lambda_S(0)$] of the scalar sector of the minimal standard model in perturbation theory. The nonminimal coupling to the gravitational field has been kept small with no suppression of the Higgs propagator, $s(t) = 1.0$. The constraints obtained apply up to $t = 38$ which is slightly larger than the reduced Planck mass. No allowed parameter space remains for $\lambda_S(0) \geq 0.23$.
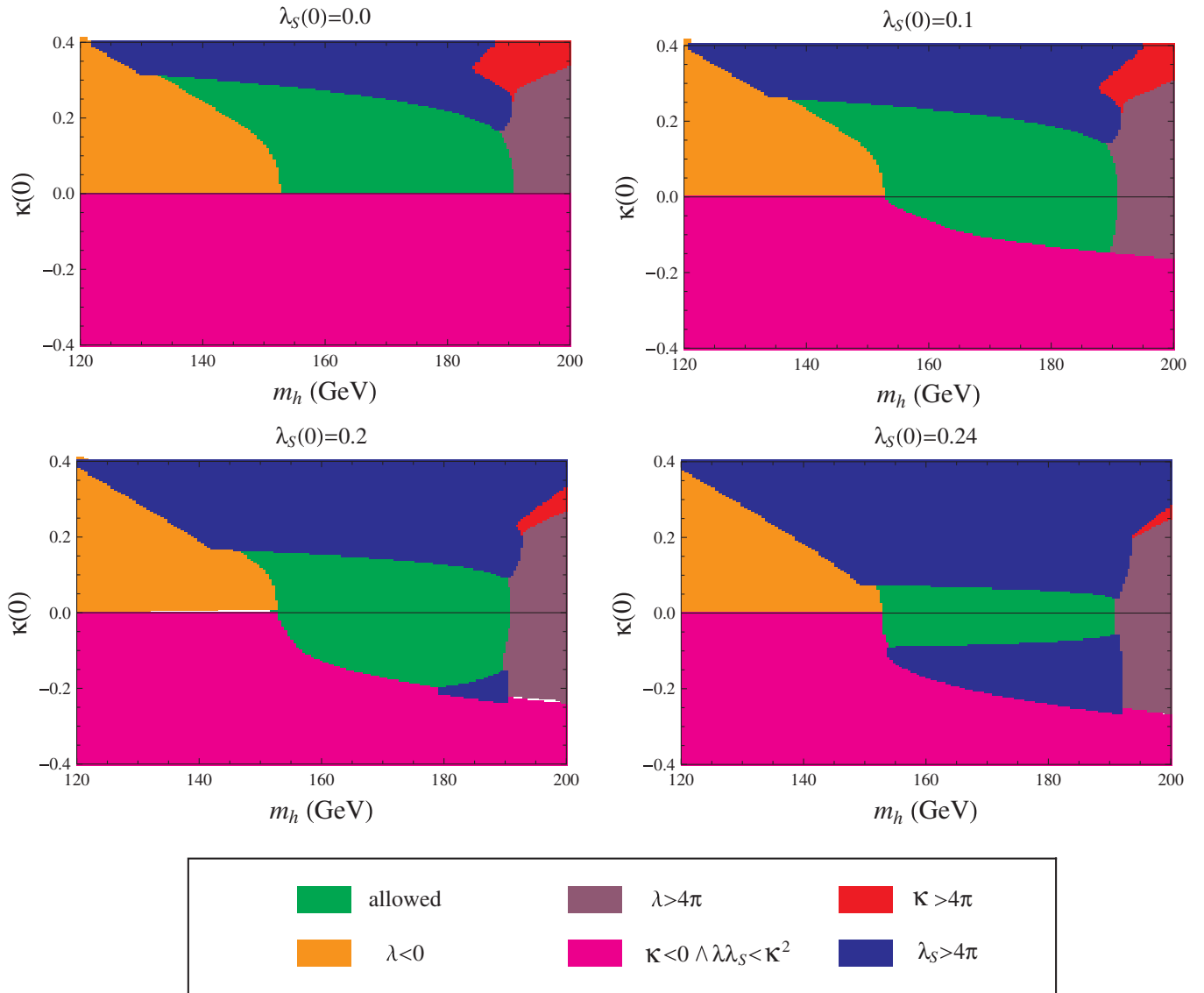
FIG. 10 (color online).   The vacuum stability and triviality constraints are applied to the parameter space of the scalar sector of the minimal standard model with large nonminimal coupling to the gravitational field, $\xi(0) = 10^4$. The Higgs propagator is suppressed with the suppression factor given in Eq. (A2) and the constraints apply to scales up to those typical of the onset of inflation, $t = 34.5$. No allowed parameter space remains for $\lambda_S(0) \gtrsim 0.25$.

when compared with the one-loop result in the special case $\lambda_S = 0$ and $\kappa = 0$ presented here.

In the next panel, Fig. 10, the parameter space constraints are determined for the case where the Higgs propagator is suppressed and the vacuum stability and triviality bounds are imposed up to the typical scale for the onset of inflation, $t = 34.5$. Here the regions were determined with an initial value of the nonminimal gravitational coupling $\xi(0) = 10^4$ and $\xi_S(0) = 0$. The size of the regions were found to be insensitive to the value of ξ for a range of values $10^3 \leq \xi(0) \leq 10^4$. The standard model without

dark matter coupling corresponds to the $\kappa(0) = 0$ abscissa in the $\lambda_S(0) = 0$ plot. There are only minor differences in the allowed parameter space for the two different cases depicted in Figs. 9 and 10 which can be directly traced to either the nonpropagation of the Higgs field for larger t values or to the fact that the constraints are applied to a larger t value in the unsuppressed Higgs propagator case. Thus, with a suppressed Higgs propagator, somewhat larger values, $m_h \simeq 190$ GeV, are allowed (as compared to ~ 180 GeV with no suppression factor).

[1] For a review see, for example, A. R. Liddle and D. H. Lyth, *Cosmologial Inflation and Large-Scale Structure* (Cambridge University Press, Cambridge, England, 2000).

[2] A. D. Linde, *Particle Physics and Inflationary Cosmology* (Harwood, Chur, Switzerland, 1990); D. H. Lyth and A. Riotto, Phys. Rep. **314**, 1 (1999); A. Linde, Lect. Notes Phys. **738**, 1 (2008).

[3] B. L. Spokoiny, Phys. Lett. **147B**, 39 (1984).

[4] D. S. Salopek, J. R. Bond, and J. M. Bardeen, Phys. Rev. D **40**, 1753 (1989).

[5] R. Fakir and W. G. Unruh, Phys. Rev. D **41**, 1783 (1990).

[6] D. I. Kaiser, Phys. Rev. D **52**, 4295 (1995).

[7] E. Komatsu and T. Futamase, Phys. Rev. D **59**, 064029 (1999).

[8] S. Tsujikawa and B. Gumjudpai, Phys. Rev. D **69**, 123523 (2004).

[9] A. O. Barvinsky and A. Y. Kamenshchik, Phys. Lett. B **332**, 270 (1994).

[10] F. L. Bezrukov and M. Shaposhnikov, Phys. Lett. B **659**, 703 (2008).

[11] A. O. Barvinsky, A. Y. Kamenshchik, and A. A. Starobinsky, J. Cosmol. Astropart. Phys. 11 (2008) 021; F. Bezrukov, D. Gorbunov, and M. Shaposhnikov, J. Cosmol. Astropart. Phys. 06 (2009) 029.

[12] A. De Simone, M. P. Hertzberg, and F. Wilczek, Phys. Lett. B **678**, 1 (2009).

[13] F. L. Bezrukov, A. Magnin, and M. Shaposhnikov, Phys. Lett. B **675**, 88 (2009); F. Bezrukov and M. Shaposhnikov, J. High Energy Phys. 07 (2009) 089.

[14] A. O. Barvinsky, A. Y. Kamenshchik, C. Kiefer, A. A. Starobinsky, and C. Steinwachs, arXiv:0904.1698.

[15] S. T. Love, arXiv:0909.5353

[16] V. Silveira and A. Zee, Phys. Lett. **161B**, 136 (1985).

[17] J. McDonald, Phys. Rev. D **50**, 3637 (1994).

[18] C. P. Burgess, M. Pospelov, and T. ter Veldhuis, Nucl. Phys. **B619**, 709 (2001).

[19] H. Davoudiasl, R. Kitano, T. Li, and H. Murayama, Phys. Lett. B **609**, 117 (2005).

[20] X. G. He, T. Li, X. Q. Li, J. Tandean, and H. C. Tsai, Phys. Rev. D **79**, 023521 (2009).

[21] E. Ponton and L. Randall, J. High Energy Phys. 04 (2009) 080.

[22] C. E. Yaguna, J. Cosmol. Astropart. Phys. 03 (2009) 003.

[23] C. Bird, P. Jackson, R. V. Kowalewski, and M. Pospelov, Phys. Rev. Lett. **93**, 201803 (2004).

[24] V. Barger, P. Langacker, M. McCaskey, M. J. Ramsey-Musolf, and G. Shaughnessy, Phys. Rev. D **77**, 035005 (2008).

[25] X. G. He, T. Li, X. Q. Li, and H. C. Tsai, Mod. Phys. Lett. A **22**, 2121 (2007).

[26] C. P. Burgess, H. M. Lee, and M. Trott, J. High Energy Phys. 09 (2009) 103; J. L. F. Barbon and J. R. Espinosa, Phys. Rev. D **79**, 081302 (2009).

[27] G. Hinshaw *et al.* (WMAP Collaboration), Astrophys. J. Suppl. Ser. **180**, 225 (2009).

[28] C. Amsler *et al.* (Particle Data Group), Phys. Lett. B **667**, 1 (2008).

[29] J. R. Espinosa, G. F. Giudice, and A. Riotto, J. Cosmol. Astropart. Phys. 05 (2008) 002.

[30] M. C. Bento, O. Bertolami, R. Rosenfeld, and L. Teodoro, Phys. Rev. D **62**, 041302 (2000).

[31] J. McDonald, Phys. Rev. Lett. **88**, 091304 (2002).

[32] R. Barate *et al.* (LEP Working Group for Higgs boson searches and ALEPH Collaboration and DELPHI Collaboration and L3 Collaboration and OPAL Collaboration), Phys. Lett. B **565**, 61 (2003).

[33] M. W. Grunewald, J. Phys. Conf. Ser. **110**, 042008 (2008).

[34] D. Benjamin (for the CDF and DO Collaborations), arXiv:0906.1403.

[35] T. P. Cheng, E. Eichten, and L. F. Li, Phys. Rev. D **9**, 2259 (1974).

[36] A. O. Barvinsky, A. Y. Kamenshchik, and I. P. Karmazin, Phys. Rev. D **48**, 3677 (1993); A. O. Barvinsky and A. Y. Kamenshchik, Nucl. Phys. **B532**, 339 (1998).

[37] J. Ellis, J. R. Espinosa, G. F. Giudice, A. Hoecker, and A. Riotto, arXiv:0906.0954; J. R. Espinosa, G. F. Giudice, and A. Riotto, J. Cosmol. Astropart. Phys. 05 (2008) 002; Yu. F. Pirogov and O. V. Zenin, Eur. Phys. J. C **10**, 629 (1999); Yad. Fiz. **66**, 1820 (2003) [Phys. At. Nucl. **66**, 1773 (2003)].